Pergamon

Int. J. Solids Structures Vol. 32, No. 24, pp. 3669–3691, 1995

0020–7683/95 $9.50 + .00

0020–7683(95)00009–7

A MACROSCOPIC CONSTITUTIVE LAW FOR POROUS SOLIDS WITH PRESSURE-SENSITIVE MATRICES AND ITS IMPLICATIONS TO PLASTIC FLOW LOCALIZATION

H.-Y. JEONG and J. PAN
Mechanical Engineering and Applied Mechanics, The University of Michigan, Ann Arbor, MI 48109, U.S.A.

(*Received* 20 *May* 1994; *in revised form* 9 *December* 1994)

Abstract—A macroscopic yield criterion for porous solids with pressure-sensitive matrices modeled by Coulomb's yield criterion is obtained by generalizing Gurson's yield criterion with consideration of the hydrostatic yield stress for a spherical thick-walled shell and by fitting the finite element results of a voided cube. From the macroscopic yield criterion, a plastic potential function for porous solids is derived for either plastic normality or non-normality flow for pressure-sensitive matrices. In addition, the elastic relation, an evolution rule for the plastic behavior of the matrices, the consistency equation and the void volume evolution equation are presented to complete a set of constitutive relations for porous solids with rate-dependent pressure-sensitive matrices. Based on the constitutive relations, plastic flow localization is analysed for porous solids with various pressure-sensitive dilatant matrices with power-law strain hardening or with intrinsic strain softening under plane strain tension, axisymmetric tension and plane stress biaxial loading. Our numerical results indicate that the non-normality of the pressure-sensitive matrices promotes localization under plane strain tension. Under axisymmetric tension the critical strain at localization decreases significantly as the pressure sensitivity of the matrices increases. Under plane stress biaxial loading conditions, the pressure sensitivity of the matrices with normality retards localization significantly. However, the pressure sensitivity of the matrices with non-normality retards localization slightly for positive strain ratios and promotes localization slightly for negative strain ratios. Under all three deformation modes, the strain softening coupled with a moderate amount of void volume inhomogeneity is shown to have a dominant role in plastic flow localization.

1. INTRODUCTION

In contrast to the pressure-insensitive yielding assumption in classical plasticity theories, pressure-sensitive yielding has been observed for dense metals, polymers and transformation-toughened ceramics (Spitzig *et al.*, 1975, 1976; Sternstein and Ongchin, 1969; Rabinowitz *et al.*, 1970; Sauer *et al.*, 1973; Spitzig and Richmond, 1979; Reyes-Morel and Chen, 1988). The pressure-sensitive yielding has been approximately described by Coulomb's yield criterion, where yielding is dependent on a linear combination of the effective shear stress and the hydrostatic stress (Drucker and Prager, 1952). The use of Coulomb's yield criterion is intended to model the intrinsic material flow behavior in metals and polymers, and to model the phase transformation in ceramics. On the other hand, inclusions, microvoids or microcracks also result in macroscopically pressure-sensitive yielding. For example, Gurson (1975, 1977) proposed a macroscopic pressure-sensitive yield criterion for porous materials of which the matrices are modeled by the pressure-insensitive von Mises yield criterion.

Much of the research on plastic flow localization or shear band formation for pressure-sensitive materials has been targeted at metallic materials and rock masses. In steels and aluminum alloys, voids nucleate from large second phase particles at small plastic strains, and often coalesce via void sheets consisting of voids nucleated from smaller particles; see Cox and Low (1974) and Van Stone *et al.* (1974). Rudnicki and Rice (1975) analysed the localization of deformation into a shear band as an instability in the constitutive description of homogeneous deformation in pressure-sensitive dilatant materials. The analysis is motivated by the shear localization in rock masses under compressive principal stresses. The analysis is general enough and applicable to a wide variety of pressure-sensitive dilatant

materials. Yamamoto (1978) made the connection between the localization analysis of Rudnicki and Rice (1975) for pressure-sensitive dilatant materials and that based on Gurson's yield function for porous materials. Yamamoto found that it is necessary to introduce some form of initial imperfection to obtain reasonable localization strains. Later, Chu and Needleman (1980), Saje *et al.* (1982) and Pan *et al.* (1983) examined the effect of non-normality flow due to void nucleation and material rate sensitivity on the growth of a shear band from an initial imperfection based on Gurson's yield function (Gurson, 1975, 1977; Tvergaard, 1981, 1982) for porous materials.

In the plastics industry, it has been known for years that the addition of rubber particles to plastics increases the fracture toughness of plastics significantly. Rubber-modified plastics can be used as they are or as resins for composites to produce structural parts. Localization of deformation into shear (dilatational) bands in rubber-modified plastics was studied by, for example, Breuer *et al.* (1977) and Sue (1992). The shear band formation in plastics has been studied in connection with their pressure-sensitive yielding and plastic dilatancy, for example, in Argon *et al.* (1968), Bauwens (1967, 1970), Bowden and Jukes (1972) and more recently in Jeong *et al.* (1994). These studies indicate the effect of pressure-sensitive yielding and plastic dilatancy on the formation of shear band. More references on shear bands in polymers can be found in Kinloch and Young (1983). In rubber-modified plastics such as rubber-modified polyamide, poly(vinyl chloride) and epoxy, when subject to loading, the rubber particles become cavitated and massive shear yielding occurs around the cavitated particles (Ramsteiner and Heckmann, 1985; Breuer *et al.*, 1977; Yee and Pearson, 1986).

Yee and Pearson (1986) emphasized that the rubber particles in rubber-modified epoxies become cavitated before noticeable plastic deformation of the matrix, and cavitation in the rubber particles is followed by massive shear yielding of the neighboring matrix. The load-carrying capacity of the rubber particles is relatively small when compared to that of the neighboring matrix. Therefore, the load-carrying capacity of the rubber particles may be neglected and the volume occupied by the rubber particles can be regarded as the volume of voids in rubber-modified plastics. Based on this viewpoint, Lazzeri and Bucknall (1993) generalized Gurson's yield function to include the pressure sensitivity of the matrices in porous solids and analyse the effect of pressure sensitivity on the formation of cavitated shear bands (dilatational bands) in rubber-modified plastics. Their generalization of Gurson's yield function for porous solids can be regarded as qualitatively correct but without any substantiation from either experimental or analytical evidence.

We are interested in modeling the constitutive behavior of rubber-modified plastics at large plastic deformation and eventually examining the toughening theory for rubber-modified plastics. The plastic zone sizes and shapes near the tips of cracks in pressure-sensitive materials have been studied in Dong and Pan (1990), Kim and Pan (1994), and Ben Aoun and Pan (1994). The general effect of the pressure sensitivity under plane strain conditions is to shift the near-tip plastic deformation to the front of the crack tip. For transformation-toughened ceramics, the pressure sensitivity for phase transformation is quite large. Ben Aoun and Pan (1994) reported that Coulomb's phase transformation criterion with large pressure sensitivity along with the elastic behavior after the exhaustion of the phase transformation strain can sufficiently result in an elongated phase transformation zone ahead of a crack, as shown in the experiment of Yu and Shetty (1989).

In rubber-toughened plastics, the cavitation zone and the shear yielding zone under plane strain conditions are also located in front of the tip of a crack (Parker *et al.*, 1990; Pearson and Yee, 1991). Since the pressure sensitivity of the plastics is limited, it is reasonable to speculate that the extensive shear plastic deformation ahead of the tip must come from the additional macroscopic pressure sensitivity due to the small load-carrying capacity of cavitated particles. In order to use finite element methods to model the observed experimental results on the plastic zone size and shape near a crack tip and to further understand the deformation processes near a blunted crack tip or notch tip, we must first formulate a set of macroscopic constitutive relations for rubber-modified plastics. This set of constitutive relations should reflect the small load-carrying capacity of rubber particles and should be easily implemented into a finite element code. In fact, the set of constitutive relations developed in this paper has been adopted to investigate the deformation processes

near a blunted crack tip in rubber-modified epoxies. The computational results of the sizes and shapes of the cavitation zone and the shear yielding zone agree well with the experimental results (Jeong, 1992).

We assume that the shearing yielding of the matrices along with the cavitated rubber particles in rubber-modified plastics should be mainly responsible for the macroscopic plastic constitutive behavior. Because of the small load-carrying capacity of the rubber particles, we treat the volume fraction occupied by the rubber particles as the void volume fraction. It is well known that Coulomb's yield criterion can be used to model the plastic behavior of plastics. Therefore, we follow the spirit of Gurson (1975, 1977) and propose a macroscopic yield criterion for porous solids with pressure-sensitive matrices modeled by Coulomb's yield criterion. The macroscopic yield criterion reduces to Gurson's yield criterion when the matrices become pressure-insensitive and incompressible. It reduces to Coulomb's yield criterion when the void volume fractions of porous solids decrease to zero.

Our modification of Gurson's yield criterion to take into account the pressure sensitivity of the matrix is based on the solution of the hydrostatic yield stress for a spherical thick-walled shell. However, our proposed yield criterion does not adequately include the effect of the interaction between voids, especially at large void volume fractions. This results from the fact that Gurson's yield criterion and the hydrostatic yield stress were obtained for a spherical thick-walled shell model, not for a voided cube model which can be used to take into account the void interaction. It should be noted that it is not uncommon that the volume fraction of the rubber particles can go up to 20% in rubber-modified plastics. Therefore, we adopt a voided cube model and use the finite element method to compute the macroscopic stresses causing massive plastic deformation of the cube under various multiaxial loading conditions, with the matrix being modeled as an elastic–perfectly plastic material. The proposed yield criterion is then modified to fit the finite element results.

It is noteworthy that experiments (Spitzig *et al.*, 1975, 1976; Spitzig and Richmond, 1979) for several steels and polymers show much lower plastic volume increases than those predicted by the normality flow rule. Rudnicki and Rice (1975) studied plastic flow localization for non-porous pressure-sensitive materials and demonstrated the influence of non-normality on localization. In this paper, we also model the plastic non-normality of the pressure-sensitive matrices by a plastic potential function which is different from the yield function. This plastic potential function is obtained by replacing the pressure sensitivity factor in the yield function with the dilatancy factor and then finding a fictitious flow stress such that the current stress state is located on the plastic potential surface in the stress space. Based on the plastic potential function and the plastic work equivalence, the normality and non-normality flow rules can be formulated. Note that the volume increase or lack of volume increase of the pressure-sensitive matrices, as determined by either normality or non-normality, plays an important role in void growth. This will be detailed later.

Finally, we present the elastic relation, an evolution rule for the plastic behavior of the matrices, the consistency equation and the void volume evolution equation to complete a set of constitutive relations for porous solids with rate-dependent pressure-sensitive matrices. It is well known that some polymers show strain softening and subsequent hardening behavior, for example, see Haward (1973, 1993), as well as strain-rate sensitivity, for example, see Bowden (1973) and Yee and Pearson (1986). Motivated by the experimental results of strain-rate sensitivity in a power-law form for poly(vinyl chloride) and high density polyethylene (G'Sell and Jonas, 1979), we take a simple power law to model the material strain-rate sensitivity from the phenomenological viewpoint. Moreover, we propose an evolution equation for the average flow stress of the matrix with the initial strain softening and subsequent hardening. After we formulate a complete set of constitutive relations, we examine the shear localization due to void volume inhomogeneity for three deformation modes: plane strain tension, axisymmetric tension and plane stress biaxial loading. In our localization analysis, we try to achieve two limited research goals. First, we examine the implications of the pressure sensitivity, plastic dilatancy, and non-normality flow of the matrix to shear localization, by comparing with the results of the traditional plastic localization analyses for porous solids with power-law strain hardening, pressure-insensitive, incompressible matrices. Secondly, we examine the implication of the initial strain softening

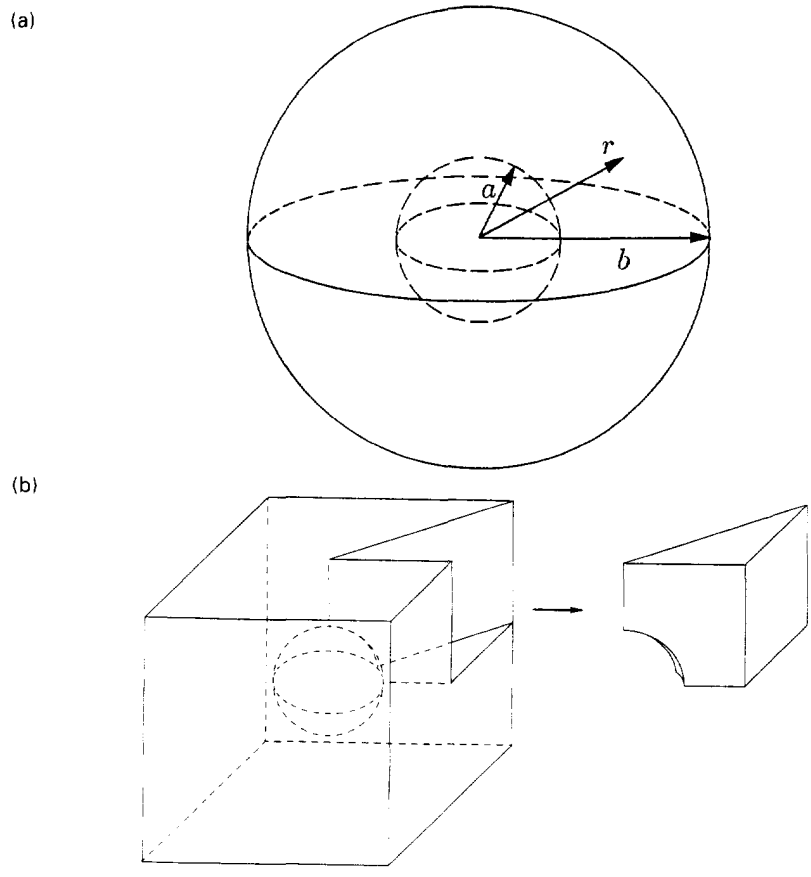

Fig. 1. (a) A spherical thick-walled shell model. (b) A voided cube model.

to shear localization. It should be noted that the subsequent strain hardening behavior stabilizes flow localization in polymers, for example, see G'Sell and Jonas' (1979). The numerical results under the three deformation modes are presented and discussed.

2. A MACROSCOPIC YIELD CRITERION

We idealize a porous material as an isotropic pressure-sensitive matrix containing a periodic array of spherical voids. Then we can model the porous material approximately as an aggregate of spherical thick-walled shells or exactly as an aggregate of voided cubes, shown in Fig. 1. The cube model is more realistic than the shell model not only because it can fill all of the space of the porous material but also because it can be used to take into account the interaction between voids. In order to construct a macroscopic yield criterion, we tentatively assume that the matrix is rigid–perfectly plastic. We also assume that the pressure sensitivity factor of the matrix is independent of the amount of plastic deformation.

As discussed by Spitzig *et al.* (1975, 1976), Sternstein and Ongchin (1969), and Spitzig and Richmond (1979), the pressure-sensitive yielding of the matrix can be modeled by Coulomb's yield criterion as

$$\tau_e + \mu\sigma_m = \tau_o \quad \text{or} \quad \sigma_e + \mu'\sigma_m = \sigma_o, \tag{1}$$

where μ is the pressure sensitivity factor, τ_o is the generalized shear flow stress, and μ' and σ_o are $\sqrt{3}\,\mu$ and $\sqrt{3}\,\tau_o$, respectively. The effective shear stress τ_e, the effective tensile stress σ_e and the mean stress σ_m are given as

$$\sigma_m = \tfrac{1}{3}\boldsymbol{\sigma} : \mathbf{I},$$
$$\boldsymbol{\sigma}' = \boldsymbol{\sigma} - \sigma_m \mathbf{I},$$
$$\tau_e = \left(\frac{\boldsymbol{\sigma}' : \boldsymbol{\sigma}'}{2}\right)^{1/2},$$
$$\sigma_e = \sqrt{3}\,\tau_e. \tag{2}$$

where $\boldsymbol{\sigma}$ is the Cauchy stress tensor, $\boldsymbol{\sigma}'$ is the deviatoric stress tensor, $\mathbf{I}$ is the identity tensor and ":" denotes the scalar product of two tensors.

Since the matrix is assumed to be perfectly plastic in this section, the generalized shear flow stress τ_o and the generalized tensile flow stress σ_o are constant throughout plastic deformation. Note that Coulomb's yield criterion in eqn (1) reduces to the von Mises yield criterion when μ becomes zero. For several steels (HY-80, maraging, 4310 and 4330 steels), Spitzig *et al.* (1975, 1976) showed that the values of μ lie between 0.014 and 0.064. For polymers, Kinloch and Young (1983) reported that the values of μ lie between 0.10 and 0.25. For zirconia-containing ceramics, Chen (1991) showed that the values of μ for phase transformation are 0.55 and 0.77 for Mg-PSZ and Ce-TZP, respectively. Yu and Shetty (1989) reported that the value of μ for phase transformation can go up to 0.93 for Ce-TZP.

Inclusions, microvoids or microcracks, even in a pressure-insensitive matrix, result in macroscopically pressure-sensitive yielding. Idealizing a porous material as a spherical thick-walled shell shown in Fig. 1(a), Gurson (1975, 1977) carried out an upper bound analysis and suggested an approximate yield criterion for a porous material of which the matrix is pressure-insensitive:

$$\Phi_G(\boldsymbol{\Sigma}, \sigma_o, f) = \left(\frac{\Sigma_e}{\sigma_o}\right)^2 + 2f\cosh\left(\frac{3\Sigma_m}{2\sigma_o}\right) - 1 - f^2 = 0, \tag{3}$$

where f is the void volume fraction of the porous material and $\boldsymbol{\Sigma}$ is the macroscopic Cauchy stress acting on the porous material. In eqn (3), Σ_e and Σ_m are the macroscopic effective tensile stress and the macroscopic hydrostatic stress, respectively, which are defined as

$$\Sigma_m = \tfrac{1}{3}\boldsymbol{\Sigma} : \mathbf{I},$$
$$\boldsymbol{\Sigma}' = \boldsymbol{\Sigma} - \Sigma_m \mathbf{I},$$
$$\Sigma_e = \left(\frac{3\boldsymbol{\Sigma}' : \boldsymbol{\Sigma}'}{2}\right)^{1/2} \tag{4}$$

where $\boldsymbol{\Sigma}'$ represents the macroscopic deviatoric Cauchy stress.

Since a kinematically admissible velocity field satisfying plastic normality has not been found for a spherical thick-walled shell of which the matrix is pressure-sensitive, the upper bound approach of Gurson (1975, 1977) cannot be followed here. Instead, we employ the equilibrium equation and Coulomb's yield criterion, and derive the hydrostatic yield stress $(\Sigma_m)_y$ for the spherical thick-walled shell under fully yielded conditions as

$$(\Sigma_m)_y = \frac{\sigma_o}{\mu'}(1 - f^{2\mu'/(3+2\mu')}). \tag{5}$$

The detailed derivation is given in Appendix 1. When μ becomes zero, $(\Sigma_m)_y$ given in eqn (5) equals $-\frac{2}{3}\sigma_o \log f$, which is the same hydrostatic yield stress as that of Gurson's yield criterion under purely hydrostatic stress.

The macroscopic yield criterion for porous solids with pressure-sensitive matrices should reduce to Gurson's yield criterion in eqn (3) when the matrices becomes pressure-insensitive, and it should reduce to Coulomb's yield criterion in eqn (1) when the void

volume fraction of the porous solids becomes zero. The macroscopic yield criterion under purely hydrostatic stress should also give a hydrostatic yield stress very close to $(\Sigma_m)_y$ given in eqn (5). Based on these requirements, we suggest the following yield criterion:

$$\Phi_f(\mathbf{\Sigma}, \sigma_o, f, \mu') = \left(\frac{\Sigma_e + \mu'\Sigma_m}{\sigma_o}\right)^2 + 2f\cosh\left[\frac{3+\mu'}{2\mu'}\log\left(1-\mu'\frac{\Sigma_m}{\sigma_o}\right)\right] - 1 - f^2 = 0. \tag{6}$$

With resort to L'Hospital's rule, the yield criterion Φ_f can be shown to become Gurson's yield criterion as μ approaches zero. Obviously, the yield criterion Φ_f reduces to Coulomb's yield criterion when f is zero.

However, the yield criterion Φ_f, a generalized version of Gurson's yield criterion, does not adequately include the effect of the interaction between voids, especially at large void volume fractions. This is not unexpected because Gurson's yield criterion in eqn (3) and the hydrostatic yield stress given in eqn (5) were obtained for the spherical thick-walled shell model, not for the cube model. In order to compensate for the error due to void interaction in the yield criterion Φ_f, finite element computations for the cube model shown in Fig. 1(b) are performed by using ABAQUS (Hibbitt *et al.*, 1992). Because the loading we consider here is axisymmetric and the shape of the cube is symmetric, it is sufficient to analyse only one-sixteenth of the cube, as in Hom and McMeeking (1989).

All faces of this part of the cube are constrained to have zero normal displacements except the right-side and top faces which have uniform normal displacements. The void surface of the part is specified to have zero traction. The matrix of the cube is modeled as an elastic–perfectly plastic material with Poisson's ratio ν of 0.3 and the ratio of the generalized tensile flow stress σ_o to Young's modulus E, σ_o/E, of 2×10^{-3}. With a small value of σ_o/E, the matrix behavior becomes almost rigid–perfectly plastic. The finite element model consists of 1015 C3D8R elements (8 node elements with a reduced integration scheme) and 1344 nodal points. The macroscopic effective tensile stress Σ_e and the macroscopic hydrostatic stress Σ_m are determined at the load where massive plastic deformation occurs. These two invariants, after being normalized by σ_o, are shown by the open symbols in Fig. 2 for several initial void volume fractions ($f = 0.01, 0.05, 0.10$ and 0.20) and pressure sensitivity factors ($\mu = 0.0, 0.1, 0.2$ and 0.3). The ranges of these parameters were chosen to represent those for typical rubber-toughened plastics.

Tvergaard (1981, 1982) introduced three parameters ($q_1 = 1.5$, $q_2 = 1.0$ and $q_3 = 2.25$) into Gurson's yield criterion by comparing the plastic flow localization results of his finite element computations with those of a continuum model based on Gurson's yield criterion. To obtain the best fit to our finite element results, we include three parameters $q_1 = 1.35$, $q_2 = 0.95$ and $q_3 = 1.35$ in the yield criterion Φ_f and arrive at a new yield criterion Φ:

$$\Phi(\mathbf{\Sigma}, \sigma_o, f, \mu') = \left(\frac{\Sigma_e + \mu'\Sigma_m}{\sigma_o}\right)^2 + 2q_1 f\cosh\left[q_2\frac{3+\mu'}{2\mu'}\log\left(1-\mu'\frac{\Sigma_m}{\sigma_o}\right)\right] - 1 - q_3 f^2 = 0. \tag{7}$$

It should be noted that the values of our q_1, q_2 and q_3 are different from those of Tvergaard.

We show the yield criterion Φ by the curves in Fig. 2, along with the open symbols from the finite element results. We also show the hydrostatic yield stress $(\Sigma_m)_y$ given by eqn (5) by the solid symbols in the figure. Since the yield criterion Φ_f under purely hydrostatic stress gives a value very close to the hydrostatic yield stress $(\Sigma_m)_y$, the difference between the yield criterion Φ under purely hydrostatic stress and $(\Sigma_m)_y$ is the amount of correction resulting from the parameters q_1, q_2 and q_3. Note that the yield criterion Φ is in good agreement with the finite element results for a wide range of void volume fractions and pressure sensitivity factors. However, the yield criterion Φ is not applicable to a negative hydrostatic stress state.

In order to establish the plastic flow rule, a plastic potential function needs to be defined. As discussed in Appendix 2, a plastic potential function in eqn (A18) for a pressure-sensitive matrix is obtained by replacing the pressure sensitivity factor μ in Coulomb's yield criterion in eqn (A14) with the dilatancy factor β and finding a fictitious generalized shear flow stress τ_p such that the current stress state is located on the plastic potential surface in the stress space. The yield criterion Φ in eqn (7) is assumed to be valid through plastic deformation. Then a plastic potential function for a porous material, $\Phi_p(\mathbf{\Sigma}, \sigma_p, f, \beta')$, can be obtained in the same way from the yield criterion $\Phi(\mathbf{\Sigma}, \sigma_o, f, \mu')$ by replacing μ' with β' and finding a fictitious generalized tensile flow stress σ_p. Here, β' is $\sqrt{3}\beta$.

The yield function and the plastic potential function are schematically drawn in Fig. 3, where $\mathbf{d}^p$ represents the plastic part of the rate of deformation tensor of the matrix, $\mathbf{D}^p$ represents the plastic part of the rate of deformation tensor of the porous material, $\dot{\gamma}_e^p$ is the effective shear plastic strain rate of the matrix, D_e^p is the effective tensile plastic strain rate of the porous material, and "tr" denotes the trace of a tensor. When μ (or μ') is equal to β (or β'), the plastic potential function becomes the same as the corresponding yield criterion and plastic normality occurs. It should be noted that other forms of plastic potential functions for porous solids with rate-dependent pressure-insensitive matrices are given and discussed in Haghi and Anand (1992).

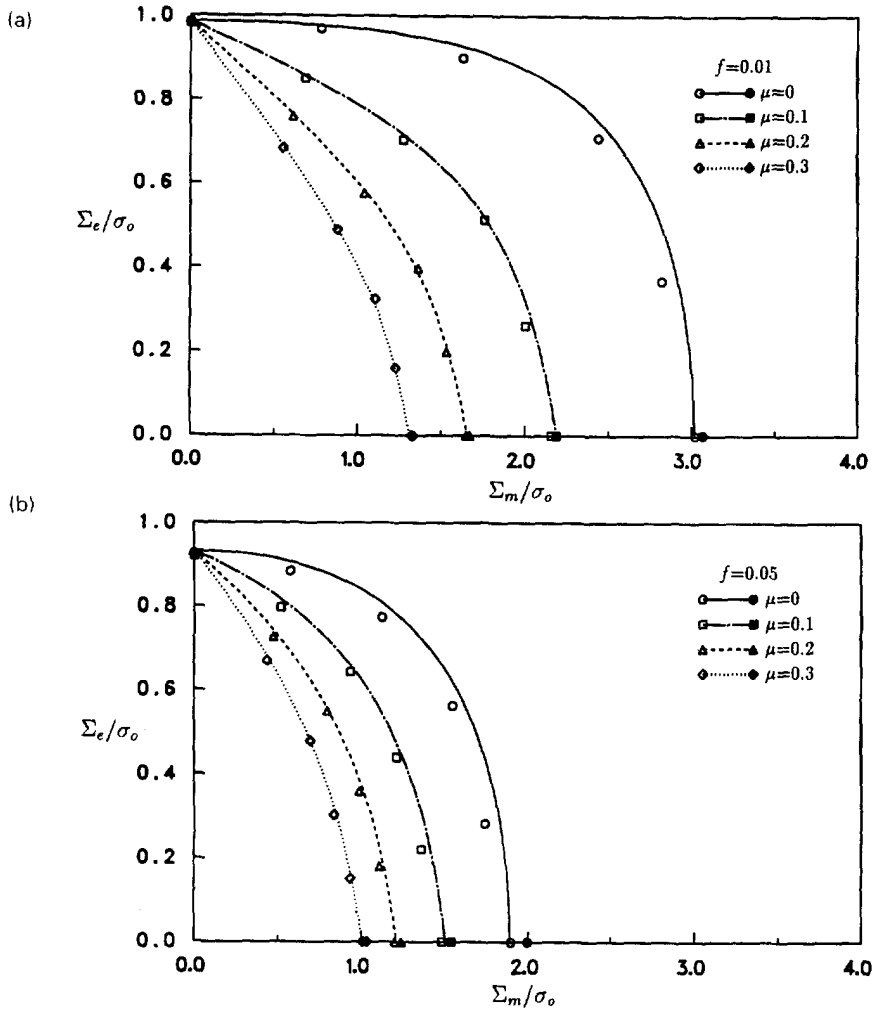

Fig. 2. Yield criteria Φ (curves), finite element results (open symbols) for the cube model, and hydrostatic yield stresses (Σ_m), (solid symbols) for the shell model for: (a) $f = 0.01$; (b) $f = 0.05$; (c) $f = 0.10$; (d) $f = 0.20$.

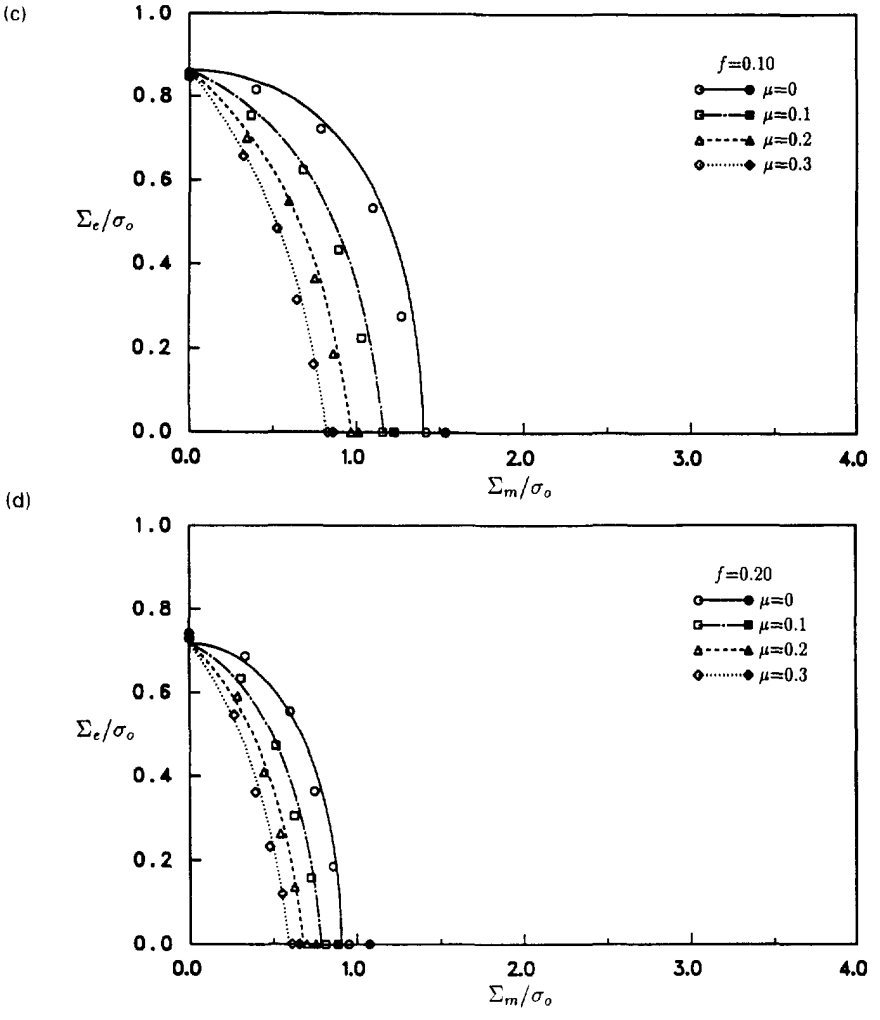

Fig. 2. (*Continued*).

3. CONSTITUTIVE RELATIONS

In this section, the constitutive relations for porous solids with rate-dependent pressure-sensitive matrices will be formulated based on the macroscopic yield criterion and the plastic potential function constructed in the previous section. Although the macroscopic yield criterion and the plastic potential function were derived for porous solids with rate-independent rigid–perfectly plastic matrices, they are assumed to be approximately valid for porous solids with rate-dependent hardening/softening matrices.

In general, the rate of deformation tensor, $\mathbf{D}$, can be decomposed into an elastic part $\mathbf{D}^e$ and a plastic part $\mathbf{D}^p$:

$$\mathbf{D} = \mathbf{D}^e + \mathbf{D}^p. \tag{8}$$

When the void volume fraction f is too large to be ignored in determining the elastic moduli of a porous material, we employ the self-consistent model with the average stress scheme of Tandon and Weng (1988). Young's modulus E^* and Poisson's ratio ν^* for a porous material are derived from Young's modulus E and Poisson's ratio ν of the matrix of the porous material as

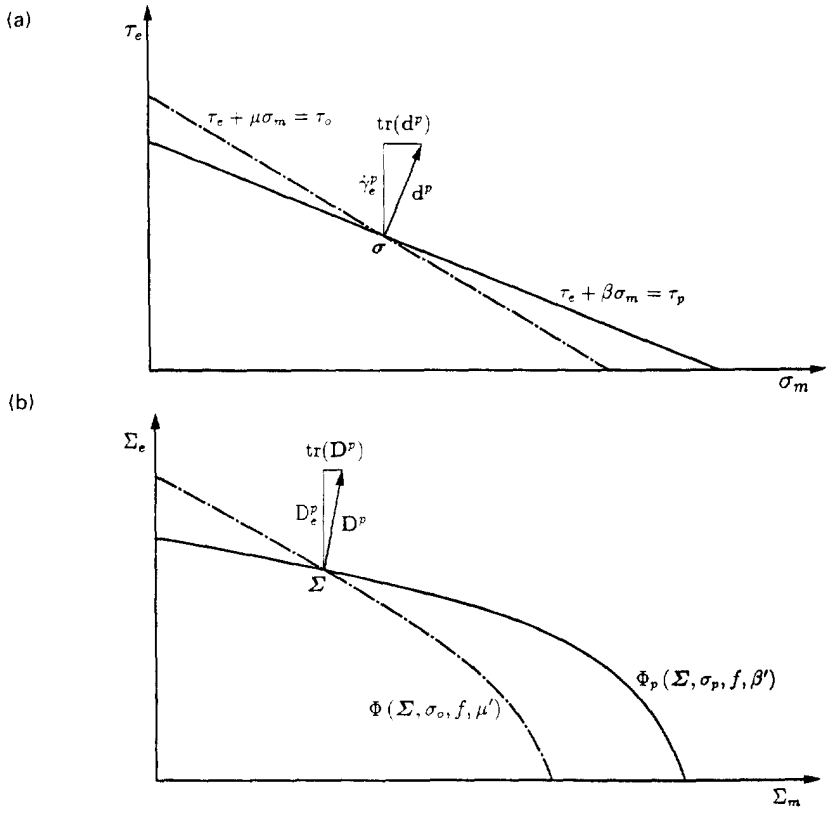

Fig. 3. Yield function and plastic potential function for: (a) a pressure-sensitive matrix; (b) a porous solid with a pressure-sensitive matrix.

$$E^* = \frac{2E(7-5\nu)(1-f)}{14-10\nu+f(1+\nu)(13-15\nu)}, \tag{9}$$

$$\nu^* = \frac{\nu(14-10\nu)+f(1+\nu)(3-5\nu)}{14-10\nu+f(1+\nu)(13-15\nu)}. \tag{10}$$

With the elastic moduli E^* and ν^*, the elastic part $\mathbf{D}^e$ is related to the Jaumann rate of the macroscopic Cauchy stress, $\hat{\boldsymbol{\Sigma}}$, as

$$\mathbf{D}^e = \frac{1}{E^*}[(1+\nu^*)\hat{\boldsymbol{\Sigma}} - \nu^*(\hat{\boldsymbol{\Sigma}}:\mathbf{I})\mathbf{I}] = \mathbf{L}^{-1}:\hat{\boldsymbol{\Sigma}}, \tag{11}$$

where $\mathbf{L}$ is the elastic modulus tensor of the porous material.

Moreover, the covariant components of the plastic part $\mathbf{D}^p$ are related to the partial derivatives of the plastic potential function Φ_p with respect to the corresponding contravariant components of the macroscopic Cauchy stress tensor $\boldsymbol{\Sigma}$ as

$$D^p_{\alpha\beta} = \dot{\Lambda}\frac{\partial \Phi_p}{\partial \Sigma^{\alpha\beta}}. \tag{12}$$

where $\dot{\Lambda}$ is a proportionality factor. In this paper, Latin indices range from 1 to 3 and Greek indices range from 1 to 2, and summation convention is adopted for repeated indices. The equivalent plastic work rate expression for a porous material is (see Appendix 2)

$$\boldsymbol{\Sigma} : \mathbf{D}^p = (1-f)\sigma_p \dot{\varepsilon}_e^p, \tag{13}$$

where σ_p is a fictitious generalized tensile flow stress of the matrix and $\dot{\varepsilon}_e^p$ is the effective tensile plastic strain rate of the matrix. Combining eqns (12) and (13) gives the proportionality factor $\dot{\Lambda}$ as

$$\dot{\Lambda} = \frac{(1-f)\sigma_p \dot{\varepsilon}_e^p}{\Sigma^{ij} \dfrac{\partial \Phi_p}{\partial \Sigma^{ij}}}. \tag{14}$$

Substituting eqns (11) and (12) into eqn (8) results in

$$\hat{\boldsymbol{\Sigma}} = \mathbf{L} : \mathbf{D} - \dot{\Lambda}\mathbf{P}, \tag{15}$$

where

$$P^{ij} = L^{ijkl} \frac{\partial \Phi_p}{\partial \Sigma^{kl}}. \tag{16}$$

Some polymers show intrinsic strain softening and subsequent hardening behavior (Haward, 1973, 1993) as well as strain-rate sensitivity (Bowden, 1973; Yee and Pearson, 1986). G'Sell and Jonas (1979) showed the strain-rate dependence in a power-law form for poly(vinyl chloride) and high density polyethylene. We take this simple power law with the strain-rate hardening exponent m:

$$\dot{\varepsilon}_e^p = \dot{\varepsilon}_r \left[\frac{\sigma_o}{g(\varepsilon_e^p)} \right]^{1/m}, \tag{17}$$

where $\dot{\varepsilon}_r$ is the reference tensile plastic strain rate, and the function $g(\varepsilon_e^p)$ equals the generalized tensile flow stress σ_o of the matrix when $\dot{\varepsilon}_e^p = \dot{\varepsilon}_r$. The form of $g(\varepsilon_e^p)$ given by G'Sell and Jonas is $g(\varepsilon_e^p) = K \exp(M\varepsilon_e^{p2})$, where K and M are material constants. The rate sensitivities for the two materials are in the range of 0.02–0.06 and play a relatively minor role in flow localization (G'Sell and Jonas, 1979).

The model materials that we work with are epoxies. It should be noted that there are many different epoxies. A variety of the stress–strain behaviors, from extremely brittle to fairly ductile, can be obtained by varying the chemical composition and processing conditions. For example, the epoxy of Yee and Pearson (1986) does yield and exhibits intrinsic strain softening in tensile tests. Kinloch *et al.* (1987) obtained the stress–strain curves of epoxies up to strain of 0.75 by plane strain compression tests. Huang and Kinloch (1992) also fitted an experimental stress–strain curve of epoxies by a piecewise curve to catch the strain softening and subsequent hardening behavior of epoxies up to strain of 0.75. Huang and Kinloch (1992) used the piecewise stress–strain curve to study the deformation pattern of the matrix in rubber-modified epoxies. Here, we propose a function for $g(\varepsilon_e^p)$ to model the initial strain softening and subsequent hardening behavior at large plastic strains for plastics. This function $g(\varepsilon_e^p)$ has the hardening exponent N, the softening–hardening exponent N_1, and two coefficients C_1 and C_2 as

$$g(\varepsilon_e^p) = \sigma_y \left[\left(\frac{\varepsilon_e^p}{\varepsilon_y} + 1 \right)^N + C_1 \left(\frac{\varepsilon_e^p}{\varepsilon_y} \right)^{N_1} \log\left(C_2 \frac{\varepsilon_e^p}{\varepsilon_y} \right) \right]. \tag{18}$$

Here, σ_y is $\sqrt{3}\tau_y$, where τ_y is the yield stress in shear at the reference shear plastic strain rate $\dot{\gamma}_r (= \sqrt{3}\dot{\varepsilon}_r)$, and ε_y is σ_y/E. When C_1 is equal to zero, eqn (18) reduces to the usual

power-law strain hardening relation. One can fit an experimental stress–strain curve by varying the values of N, N_1, C_1 and C_2.

It should be noted that the deformation of the matrix in a unit cell model is not uniform. As in the work of Gurson (1975, 1977), σ_y and $\bar{\varepsilon}_c^p$ on the right hand side of eqn (13) represent the average flow stress and plastic strain rate of the matrix for evaluation of the macroscopic plastic dissipation rate. Equation (18) is merely a convenient form to represent the average flow stress of the matrix, including the intrinsic strain softening and subsequent hardening behavior of plastics, so that we can qualitatively understand the effect of the strain softening on flow localization. For poly(vinyl chloride) and high density polyethylene, $g(\bar{\varepsilon}_c^p) = K\exp(M\bar{\varepsilon}_c^{p2})$ with the corresponding material constants should be adopted from the phenomenological viewpoint. A three-dimensional constitutive law was given by Boyce *et al.* (1988) for glassy polymers based on the macromolecular structure and micromechanisms of plastic flow. Their constitutive law can take into account the strain rate, temperature, and pressure dependence of the plastic behavior of glassy polymers. It is possible that their model can be adopted to give the relation of the average flow stress, plastic strain and plastic strain rate of the matrix in an approximate sense with some assumption of the dependence of the average back stress tensor on the average deformation of the matrix. The material constants for their model are available for poly(methyl methacrylate) (PMMA).

The increase of the void volume fraction arises from the growth of existing voids and from the nucleation of voids. The plastic dilatancy of the pressure-sensitive matrix suppresses the void growth that would occur without it by $(1-f)\beta'\bar{\varepsilon}_c^p$. Thus, it plays an important role in void growth, as we pointed out earlier. For the nucleation of voids, we adopt two models: one is the plastic strain controlled nucleation model suggested by Gurson (1975, 1977) based on Gurland's experimental data (1972), and the other is the stress controlled nucleation model discussed in Argon and Im (1975). Chu and Needleman (1980) used the normal distributions to implement these nucleation models. Therefore, the increase rate of the void volume fraction can be expressed as

$$\dot{f} = \dot{f}_{\text{growth}} + \dot{f}_{\text{nucleation}} = (1-f)[\text{tr}(\mathbf{D}^p) - \beta'\dot{\bar{\varepsilon}}_c^p] + A\dot{\bar{\varepsilon}}_c^p + B(\dot{\sigma}_o + \dot{\Sigma}_m), \tag{19}$$

where

$$A = \frac{f_A}{s\sqrt{2\pi}}\exp\left[-\frac{1}{2}\left(\frac{\bar{\varepsilon}_c^p - \varepsilon_N}{s}\right)^2\right] \quad \text{for} \quad \bar{\varepsilon}_c^p > (\bar{\varepsilon}_c^p)_{\max},$$

$$B = \frac{f_B}{s\sigma_1\sqrt{2\pi}}\exp\left[-\frac{1}{2}\left(\frac{\sigma_o + \Sigma_m - \sigma_N}{s\sigma_1}\right)^2\right] \quad \text{for} \quad \sigma_o + \Sigma_m > (\sigma_o + \Sigma_m)_{\max}. \tag{20}$$

Here, f_A and f_B are the volume fractions of void nucleating particles for the plastic strain controlled nucleation model and the stress controlled nucleation model, respectively, s is the standard deviation, and ε_N and σ_N are the mean values of the normal distributions. A or B has a non-zero value only when $\bar{\varepsilon}_c^p$ or $\sigma_o + \Sigma_m$ becomes larger than its maximum value occurring in the prior deformation history.

Moreover, the consistency condition which holds during plastic deformation requires

$$\dot{\Phi} = \frac{\partial\Phi}{\partial\Sigma^{ij}}\dot{\Sigma}^{ij} + \frac{\partial\Phi}{\partial\sigma_o}\dot{\sigma}_o + \frac{\partial\Phi}{\partial f}\dot{f} = 0. \tag{21}$$

In summary, eqns (15), (17)–(19) and (21) describe the constitutive behavior of porous solids with rate-dependent pressure-sensitive matrices.

4. PLASTIC FLOW LOCALIZATION ANALYSIS

A Lagrangian formulation is employed with reference to the initial undeformed configuration. In addition, the coordinates of a material point relative to a fixed Cartesian frame in the undeformed configuration are taken as the convected coordinates. Therefore, the current base vectors $\bar{\mathbf{g}}_i$ can be expressed in terms of the deformation gradient tensor $\mathbf{F}$ and the reference base vectors $\mathbf{g}_j$ as

$$\bar{\mathbf{g}}_i = F^j{}_i \mathbf{g}_j. \tag{22}$$

The metric tensors in the reference configuration and in the current configuration are denoted by g_{ij} and $\bar{g}_{ij}$, respectively, and the corresponding conjugate metric tensors are g^{ij} and $\bar{g}^{ij}$, respectively. The determinants of the metric tensors are denoted by g and $\bar{g}$.

We employ the tangent modulus procedure of Peirce *et al.* (1984) to integrate the constitutive relation in eqn (15). Using the relation of the Jaumann rate of the Cauchy stress, $\hat{\boldsymbol{\Sigma}}$, to the convected rate of the Kirchhoff stress, $\dot{\mathbf{T}}$, and the relation of the rate of deformation $\mathbf{D}$ to the Lagrangian strain rate $\dot{\boldsymbol{\varepsilon}}$, we can rewrite the constitutive relation (15) as

$$\dot{T}^{ij} = \hat{L}^{ijkl}_{\tan} \dot{\varepsilon}_{kl} - \sqrt{\bar{g}/g}\dot{\Lambda} P^{ij}_{\tan}, \tag{23}$$

where $\hat{\mathbf{L}}_{\tan}$ and $\mathbf{P}_{\tan}$ are the modified tensors of $\mathbf{L}$ and $\mathbf{P}$. Detailed derivations can be found in our previous work (Jeong and Pan, 1992). For plane stress problems where $\dot{T}^{3i} = 0$, the constitutive relation in eqn (23) becomes

$$\dot{T}^{\alpha\beta} = \left(\hat{L}^{\alpha\beta\gamma\delta}_{\tan} - \frac{\hat{L}^{\alpha\beta 33}_{\tan} \hat{L}^{33\gamma\delta}_{\tan}}{\hat{L}^{3333}_{\tan}} \right) \dot{\varepsilon}_{\gamma\delta} - \sqrt{\bar{g}/g}\dot{\Lambda} \left(P^{\alpha\beta}_{\tan} - \frac{\hat{L}^{\alpha\beta 33}_{\tan} P^{33}_{\tan}}{\hat{L}^{3333}_{\tan}} \right). \tag{24}$$

In this plastic flow localization analysis, a thin imperfection band is assumed to exist in a material element, as shown in Fig. 4. In addition, homogeneous deformation is assumed to take place inside and outside the band throughout a deformation history. In this paper, we consider three deformation modes: plane strain tension, axisymmetric tension and plane stress biaxial loading. The deformation modes are imposed such that the x^1, x^2 and x^3 axes remain to be the principal directions. The principal values associated with the 1, 2 and 3

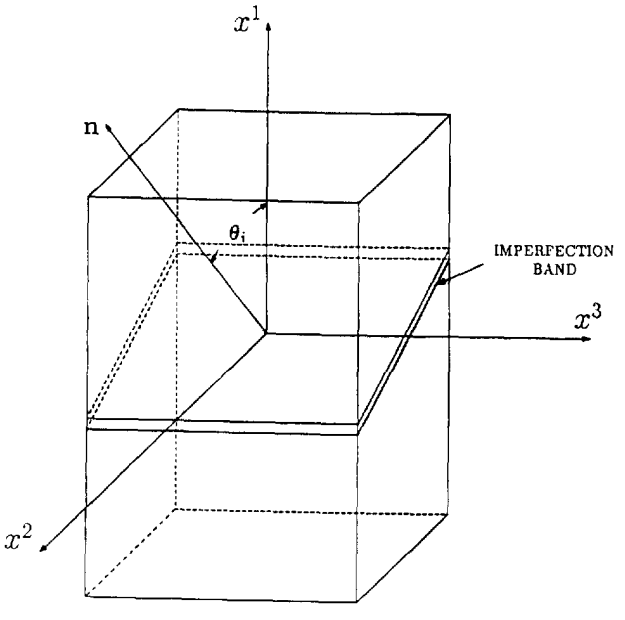

Fig. 4. A solid element having an imperfection band.

directions are denoted by $(\ )_{\mathrm{I}}$, $(\ )_{\mathrm{II}}$ and $(\ )_{\mathrm{III}}$, respectively. Furthermore, a superscript or subscript "b" represents a quantity inside the band, whereas a superscript or subscript "o" represents a quantity outside the band. Under plane strain tension, $\dot{F}^o_{\mathrm{III}}$ is equal to zero and $\dot{F}^o_{\mathrm{II}}$ is chosen such that $\dot{\Sigma}^o_{\mathrm{II}}$ vanishes. Under axisymmetric tension, $\dot{F}^o_{\mathrm{II}} = \dot{F}^o_{\mathrm{III}}$ with $\dot{\Sigma}^o_{\mathrm{II}} = \dot{\Sigma}^o_{\mathrm{III}} = 0$. These boundary conditions for plane strain tension and axisymmetric tension were originally considered by Yamamoto (1978). In simulating thin sheets under biaxial loading, a plane stress state ($\Sigma^b_{\mathrm{III}} = \Sigma^o_{\mathrm{III}} = 0$) is assumed both inside and outside the band. Only proportional straining paths are considered here, and the strain ratio outside the band ρ ($= \varepsilon^o_{\mathrm{I}}/\varepsilon^o_{\mathrm{II}}$, where $\varepsilon^o_{\mathrm{I}} = \log F^o_{\mathrm{I}}$ and $\varepsilon^o_{\mathrm{II}} = \log F^o_{\mathrm{II}}$) is prescribed to be a constant throughout a deformation history.

As deformation proceeds, compatibility (Hill, 1962; Rice, 1976) across the imperfection band interface requires

$$\mathbf{F}_b = \mathbf{F}_o + \mathbf{c} \otimes \mathbf{n}, \tag{25}$$

where $\mathbf{c}$ is a vector denoting the discontinuity across the band, $\mathbf{n}$ is a normal vector to the band in the undeformed configuration and "$\otimes$" denotes a tensor product. In addition to the compatibility, equilibrium requires that traction be continuous across the band interface. The equilibrium equation can be expressed in terms of the first Piola–Kirchhoff stress $\mathbf{S}$ and the normal vector $\mathbf{n}$ as

$$\mathbf{n} \cdot \mathbf{S}_b = \mathbf{n} \cdot \mathbf{S}_o \quad \text{with} \quad \mathbf{S} = \mathbf{F}^{-1} \cdot \mathbf{T}. \tag{26}$$

By combining the rate form of the compatibility eqn (25), the rate form of the equilibrium eqn (26) and the constitutive relation (23), a set of equations for $\dot{\mathbf{c}}$ is obtained as

$$\begin{aligned} n_i(\hat{L}^{iklp}_{\tan} F^j{}_k F^q{}_l + T^{ip} g^{jq})_b n_p \dot{c}_q = {} & n_i(F^j{}_k \sqrt{\bar{g}/g}\dot{\Lambda} P^{ik}_{\tan})_b - n_i(F^j{}_k \sqrt{\bar{g}/g}\dot{\Lambda} P^{ik}_{\tan})_o \\ & + n_i(\hat{L}^{iklp}_{\tan} F^j{}_k F^q{}_l + T^{ip} g^{jq})_o \dot{F}^o_{qp} - n_i(\hat{L}^{iklp}_{\tan} F^j{}_k F^q{}_l + T^{ip} g^{jq})_b \dot{F}^o_{qp}. \end{aligned} \tag{27}$$

Similarly, a set of equations for $\dot{\mathbf{c}}$ under plane stress biaxial loading can be obtained.

From the prescribed deformation history outside the band $\dot{\mathbf{F}}_o$ and the initial conditions, the set of eqns (27) for $\dot{\mathbf{c}}$ can be solved incrementally to determine the deformation history inside the band. Localization is said to occur when the ratio of the strain rate inside the band to the corresponding strain rate outside the band becomes unbounded.

5. NUMERICAL RESULTS

In this section, we analyse the effects of pressure sensitivity, plastic dilatancy and strain softening on plastic flow localization. First, we take $E = 3000$ MPa, $\nu = 0.4$, $\sigma_y = 75$ MPa and $m = 0.035$ based on the material properties of the epoxy of Yee and Pearson (1986). We take a softening hardening case with $N = 0.1$, $N_1 = 1.3$, $C_1 = 0.03$ and $C_2 = 0.05$. Then we take a power-law strain hardening case with $N = 0.1$ and $C_1 = 0$ as the reference case. These two curves at $\dot{\varepsilon}^p_e = \dot{\varepsilon}_e = 0.0032\ \mathrm{s}^{-1}$ are shown in Fig. 5, where curve (a) represents the power-law strain hardening case and curve (b) represents the softening–hardening case. It should be noted that the general trend of curve (b) is quite close to those stress–strain curves of epoxies shown in Kinloch *et al.* (1987) and Huang and Kinloch (1992). Certainly one can adjust the parameters in eqn (18) or using other curve fitting functions to fit the strain softening and subsequent hardening behavior of plastics. Curve (b) in Fig. 5 shows a positive curvature at large plastic strains. This positive curvature is associated with the stabilization of flow localization, for example, see G'Sell and Jonas (1979). The strain softening of curve (b) shown in Fig. 5 cannot only affect the flow localization of the matrix in rubber-modified plastics from the microscopic viewpoint (Huang and Kinloch, 1992) but also affect the flow localization of the rubber-modified plastics as continua from the macroscopic viewpoint as we examine here.

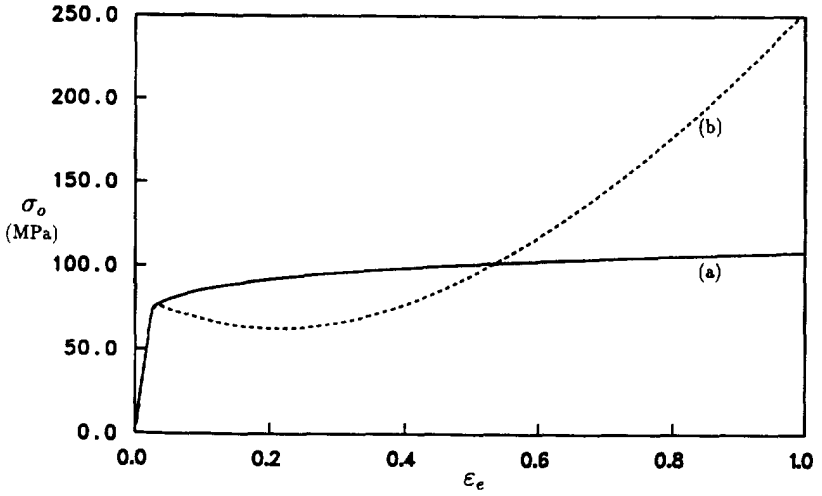

Fig. 5. Two representative stress–strain curves: (a) a power-law strain hardening curve for $N = 0.1$ and $C_1 = 0$; (b) a softening–hardening curve for $N = 0.1$, $N_1 = 1.3$, $C_1 = 0.03$ and $C_2 = 0.05$.

According to Yee and Pearson (1986), the rubber particles in rubber-modified plastics become cavitated before noticeable plastic deformation. The rubber particles can be treated approximately as voids when plastic deformation occurs in rubber-modified plastics. Typical volume fractions of the rubber particles in plastics range from 5 to 20%. We denote the initial void volume fraction outside the band by f_o and the initial void volume fraction inside the band by f_b. We take $f_o = 0.10$ and $f_b = 0.11$ for most of our numerical examples. In this paper, we consider no nucleation of voids and we prescribe $\dot{F}_1^o/F_1^o$ as $\dot{\varepsilon}_r$. Although we select the material properties of a representative rubber-modified plastic for our numerical examples, the constitutive relations and formulations for plastic flow localization in the previous sections are general and applicable to other rubber-modified plastics with the corresponding constitutive relations of the matrices.

With a pressure sensitivity factor μ and a dilatancy factor β, localization strains are computed for various initial band angles θ_i. For example, for the power-law strain hardening case with $\mu = \beta = 0$ under plane strain tension, Fig. 6 shows the logarithmic axial strains ε_1^{loc} outside the band at localization as functions of the initial band angle θ_i and the corresponding current band angle θ_c. The minimum of these curves gives the critical localization strain ε_1^{cr} at which the inception of localization is first possible. The critical

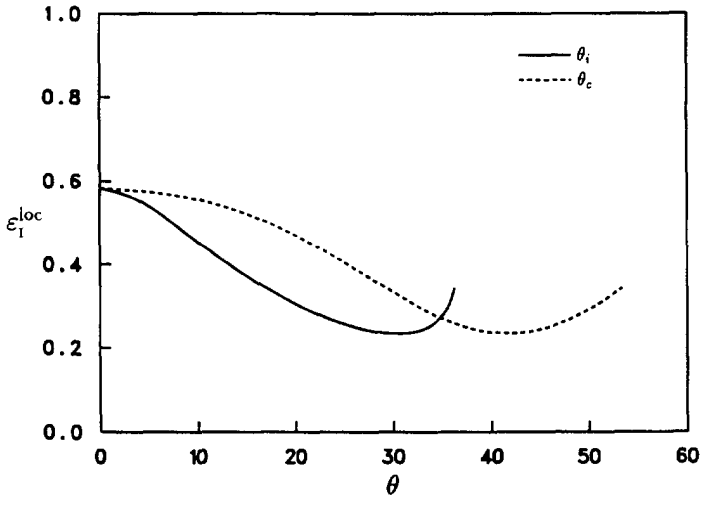

Fig. 6. Localization strains ε_1^{loc} as functions of the initial band angle θ_i and the current band angle θ_c under plane strain tension for $f_o = 0.10$, $f_b = 0.11$, $N = 0.1$, $C_1 = 0$, $\mu = 0$ and $\beta = 0$.

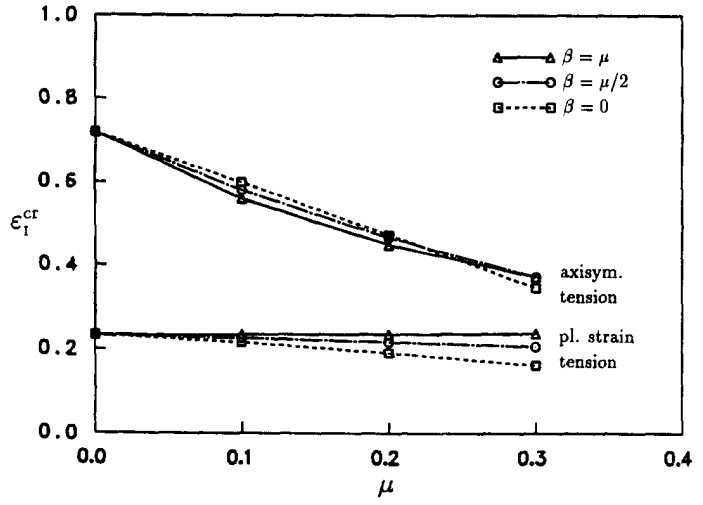

Fig. 7. Critical localization strains ε_1^{cr} under plane strain tension and axisymmetric tension for $f_a = 0.10$, $f_b = 0.11$, $N = 0.1$ and $C_1 = 0$.

localization strains for the power-law strain hardening case are plotted in Fig. 7 as functions of μ. In this figure, the lower three curves are for plane strain tension and the upper three curves are for axisymmetric tension. Only under plane strain tension with normality, the critical localization strain increases slightly as the pressure sensitivity factor increases. This is due to the volume increase of the matrix and the consequent suppression of the growth of voids. However, under plane strain tension with non-normality ($\beta = 0$ and $\beta = \mu/2$), the critical localization strain decreases as the pressure sensitivity factor increases. Under axisymmetric tension, the critical localization strain decreases significantly as the pressure sensitivity increases. The plastic dilatancy of the matrix, however, has only a slight influence on localization.

Under plane strain tension and axisymmetric tension, the difference of the critical localization strains for normality and for non-normality increases as the initial void volume fraction decreases. For example, when $f_a = 0.01$ and $f_b = 0.02$, $\varepsilon_1^{cr} = 0.481$ for $\mu = \beta = 0.3$ and $\varepsilon_1^{cr} = 0.344$ for $\mu = 0.3$ and $\beta = 0$ under plane strain tension; $\varepsilon_1^{cr} = 1.274$ for $\mu = \beta = 0.1$ and $\varepsilon_1^{cr} = 1.397$ for $\mu = 0.1$ and $\beta = 0$ under axisymmetric tension. It should be noted that for a small pressure sensitivity factor, say $\mu = 0.1$, the influence of plastic non-normality on the critical localization strain is opposite under plane strain tension and axisymmetric tension, as shown in Fig. 7: non-normality promotes localization under plane strain tension, whereas it delays localization under axisymmetric tension.

In the normalized coordinate system shown in Fig. 2, the load-carrying capacity of the porous solids decreases as the pressure sensitivity of the matrices increases and/or the void volume fraction of the porous solids increases. Furthermore, as schematically illustrated in Fig. 2, when normality applies, the pressure sensitivity of the matrices results in a larger dilatancy factor for the porous solids, $\mathrm{tr}(\mathbf{D}^p)/(\sqrt{3}D_e^p)$, when the ratio Σ_m/Σ_e is moderately small. The non-normality of the matrices results in less macroscopic plastic dilatancy, as shown in Fig. 3(b), when the ratio Σ_m/Σ_e is moderately small. In addition, the plastic dilatancy of the pressure-sensitive matrices gives the volume increase of the matrices, which suppresses the growth of the existing voids. The competition of these factors under different deformation modes gives the trends shown in Fig. 7.

For the softening–hardening case with $\mu = \beta = 0$, the logarithmic axial strains ε_1^{loc} exhibit a double-branch behavior, as shown in Figs 8 and 9 for plane strain tension and axisymmetric tension, respectively. The initial imperfection Δf $(= f_b - f_a)$ is 0.01 for the plane strain tension results and 0.03 for the axisymmetric tension results. In these figures, as the initial band angle increases from 0, the localization strain decreases slightly and increases. At certain initial band angles, however, the localization strain drops to a very small value and then increases abruptly. As the initial imperfection Δf decreases, the lower

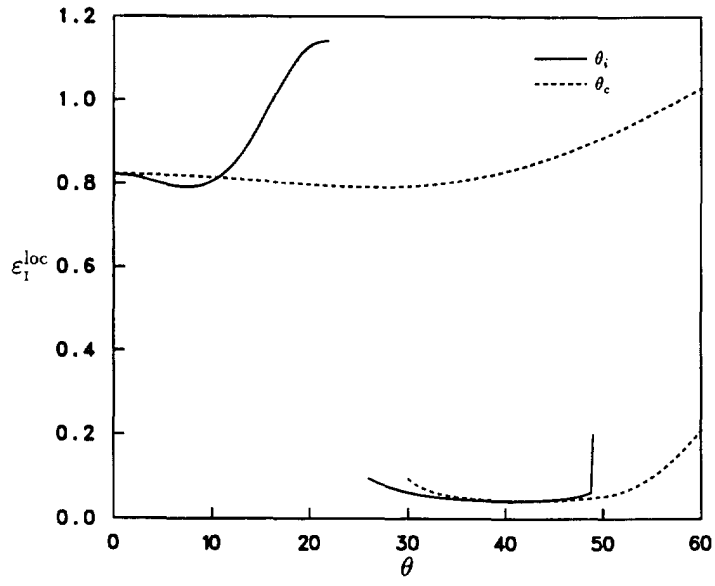

Fig. 8. Localization strains ε_1^{loc} as functions of the initial band angle θ_i and the current band angle θ_c under plane strain tension for $f_a = 0.10$, $f_b = 0.11$, $N = 0.1$, $N_1 = 1.3$, $C_1 = 0.03$, $C_2 = 0.05$, $\mu = 0$ and $\beta = 0$.

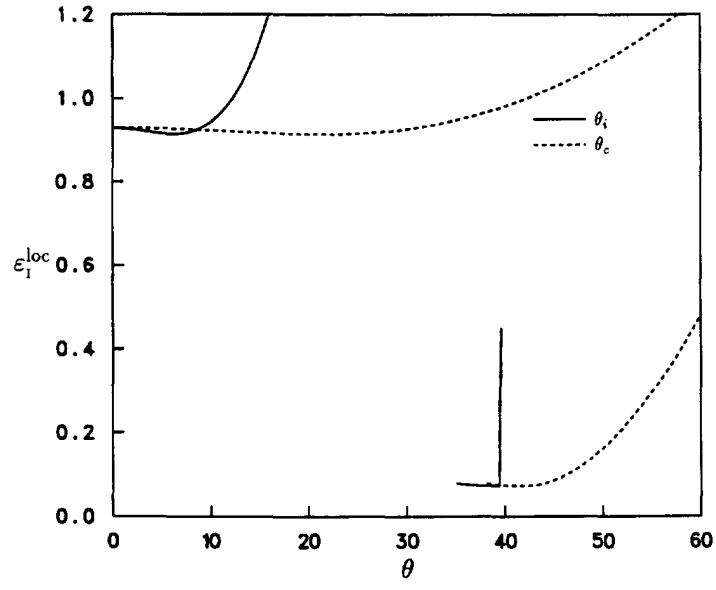

Fig. 9. Localization strains ε_1^{loc} as functions of the initial band angle θ_i and the current band angle θ_c under axisymmetric tension for $f_a = 0.10$, $f_b = 0.13$, $N = 0.1$, $N_1 = 1.3$, $C_1 = 0.03$, $C_2 = 0.05$, $\mu = 0$ and $\beta = 0$.

plateau narrows and finally disappears for the values of Δf slightly smaller than 0.001 under plane strain tension and 0.030 under axisymmetric tension. Examining the cases with different values of μ and β for the softening–hardening stress–strain behavior, we found that the critical localization strains occurring in the lower plateau are almost independent of the pressure sensitivity and plastic dilatancy. These results indicate that the strain softening has a dominant role in localization as long as the amount of initial imperfection is moderate. Especially under plane strain tension, localization is almost sure to occur near the intrinsic strain softening point, since a very small initial imperfection $\Delta f = 0.001$ can

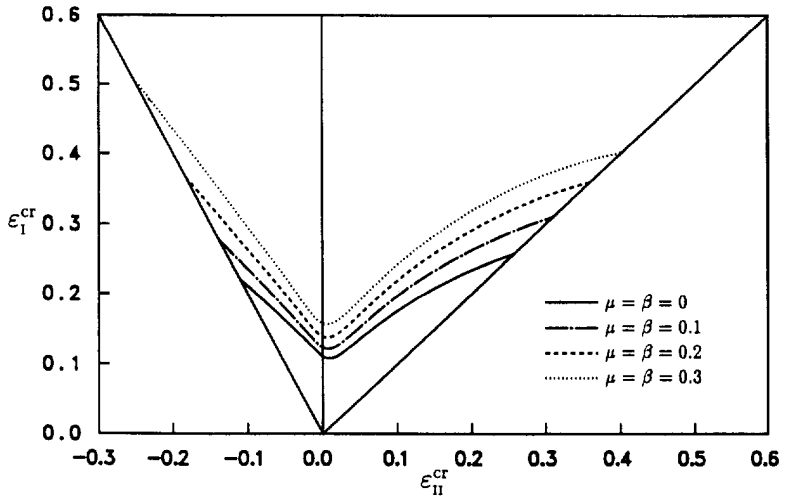

Fig. 10. Forming limit diagram with the assumption of normality for $f_a = 0.10$, $f_b = 0.11$, $N = 0.1$ and $C_1 = 0$.

exist in materials. The double-branch localization phenomenon also occurs in a rate-independent approach with a stress controlled nucleation model, as reported in Saje *et al.* (1982).

Under plane stress biaxial loading, the critical localization strains define a forming limit diagram. Figure 10 shows the forming limit diagram for the power-law strain hardening case with normality. For a given μ, the critical localization strain has a minimum around $\rho = 0$ (in-plane plane strain tension), and the critical localization strain increases as ρ increases to 1 (biaxial tension) and as ρ decreases to -0.5. The results shown in Fig. 10 indicate that the pressure-sensitive yielding of the matrix retards localized necking. This effect is especially large for ρ close to 1 and -0.5. However, for the power-law strain hardening case with non-normality of $\beta = 0$, the results shown in Fig. 11 indicate that the pressure-sensitive yielding of the matrix does not dramatically affect localized necking; it retards localized necking slightly for positive ρ, but it promotes localized necking slightly for negative ρ. For the softening–hardening case with a small initial imperfection $\Delta f = 0.01$, the results shown

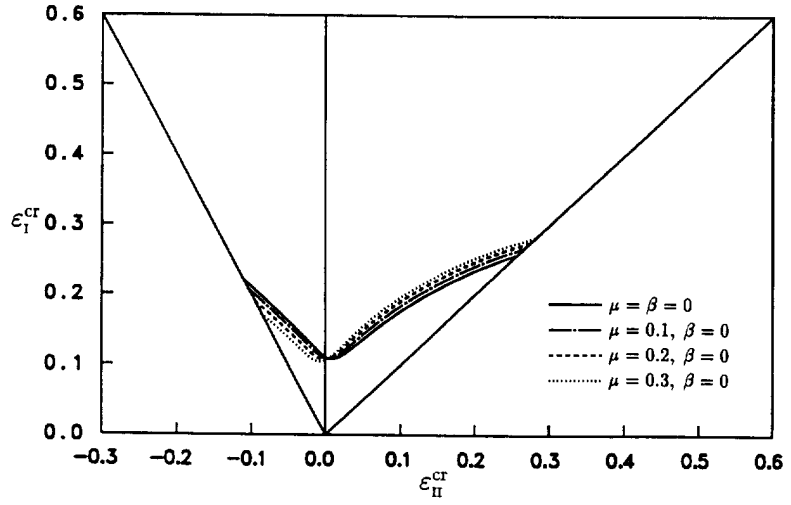

Fig. 11. Forming limit diagram with the assumption of non-normality for $f_a = 0.10$, $f_b = 0.11$, $N = 0.1$ and $C_1 = 0$.

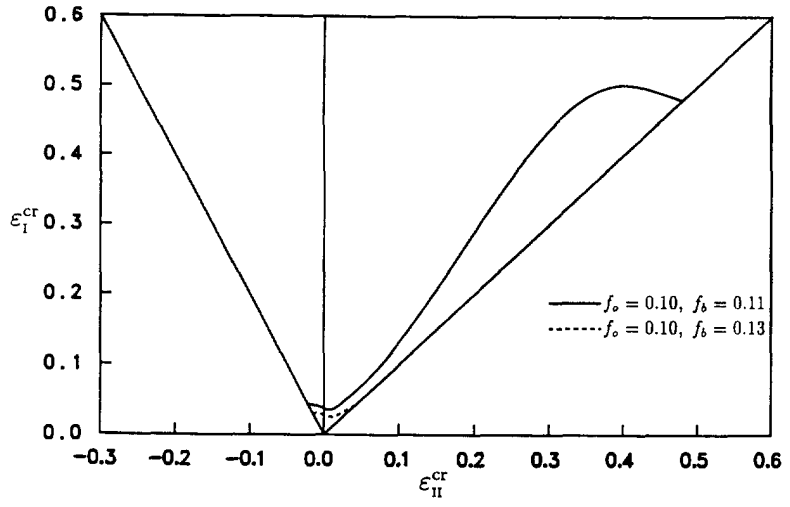

Fig. 12. Forming limit diagram for $N = 0.1$, $N_1 = 1.3$, $C_1 = 0.03$, $C_2 = 0.05$, $\mu = 0$ and $\beta = 0$.

in Fig. 12 indicate that small critical localization strains occur except for ρ close to 1. With a slightly larger initial imperfection, for example, $\Delta f = 0.03$, very small critical localization strains occur near the intrinsic strain softening point for all ρ, and the small critical localization strains do not change significantly as the pressure sensitivity or dilatancy factor varies. Similar to plane strain tension and axisymmetric tension cases, the strain softening has a dominant role in localized necking as long as the initial imperfection exceeds a critical value.

6. CONCLUSIONS AND DISCUSSION

We have formulated a set of constitutive relations for porous solids with rate-dependent pressure-sensitive matrices. Based on the constitutive relations, plastic flow localization has been analysed for porous solids with various pressure-sensitive dilatant matrices with power-law strain hardening or with intrinsic strain softening under plane strain tension, axisymmetric tension and plane stress biaxial loading.

Under plane strain tension, the pressure-sensitive yielding of the matrix with normality retards plastic flow localization slightly, but the pressure-sensitive yielding of the matrix with non-normality of $\beta = 0$ gives early plastic flow localization. This means that under plane strain tension, the plastic dilatancy of the matrix plays a major role in plastic flow localization and its influence, for example, when normality occurs, overcomes the effect of the reduction of the load-carrying capacity due to the pressure-sensitive yielding of the matrix. Under axisymmetric tension, however, the pressure-sensitive yielding of the matrix promotes plastic flow localization significantly, but the plastic dilatancy of the matrix does not affect localization as much as the pressure-sensitive yielding of the matrix does. In contrast to the plane strain tension case, the reduction of the load-carrying capacity due to the pressure-sensitive yielding of the matrix plays a major role in plastic flow localization under axisymmetric tension. Under plane stress biaxial loading, the pressure-sensitive yielding of the matrix with normality retards localized necking, but the pressure-sensitive yielding of the matrix with non-normality of $\beta = 0$ does not affect localized necking significantly.

Under all three deformation modes, the strain softening coupled with a moderate amount of initial void volume inhomogeneities gives a double-branch localization behavior, as shown in Figs 8 and 9. This indicates that the strain softening has a dominant effect on

plastic flow localization, and plastic flow localization occurs near the intrinsic strain softening point when the initial imperfection exceeds a critical value. It should be noted that the double-branch behavior in flow localization also occurs when the stress-controlled void nucleation criterion is employed in the rate-independent analysis of Saje *et al.* (1982). However, when material rate sensitivity is considered, the double-branch behavior disappears, although a substantial amount of shear deformation occurs within the band when the stress-controlled void nucleation takes place (Pan *et al.*, 1983). Here the dominant strain softening effect coupled with the rapid loss of the load-carrying capacity due to large void volume fractions overcomes the effects of the material rate sensitivity and the subsequent strain hardening for flow stabilization. Consequently, the double-branch behavior appears. The amount of strain softening can affect the critical value of the void volume fraction for the double-branch behavior. When the amount of strain softening increases, the critical void volume fraction for the double-branch behavior should decrease. The detailed stress–strain behavior for the strain softening and the subsequent strain hardening may also have some influences on the double-branch behavior, but the results on localization should be qualitatively similar to those presented here. Our results show that with strain softening it only takes a very small amount of imperfection to induce localization under plane strain conditions. This may explain the massive shear yielding ahead of a crack in the rubber-modified epoxy of Pearson and Yee (1991). This massive yielding ahead of the tip of a crack has been thought of as a major mechanism for toughening in this class of materials.

Acknowledgements—The support of this work by a Material Research Group grant funded by the National Science Foundation under grant no. DMR-8708405 at The University of Michigan is gratefully acknowledged. The partial support of the Rackham Predoctoral Fellowship of The University of Michigan to HYJ is also acknowledged. Helpful discussions with Professor A. F. Yee of The University of Michigan, Dr. D. M. Li of Exxon, and Ms. X.-W. Li of Michigan State University are greatly appreciated.

REFERENCES

Argon, A. S., Andrews, R. D., Godrick, J. A. and Whitney, W. (1968). Plastic deformation bands in glassy polystyrene. *J. Appl. Phys.* **39,** 1899–1906.

Argon, A. S. and Im, J. (1975). Separation of second phase particles in spheroidized 1045 steel, Cu-0.6pct Cr alloy, and maraging steel in plastic straining. *Metall. Trans.* **6A,** 839–851.

Bauwens, J. C. (1967). Déformation plastique des haus Polymères vitreux soumis à un Système de Constraintes quelconque. *J. Polymer Sci.: Part A-2* **5,** 1145–1156.

Bauwens, J. C. (1970). Yield condition and propagation of Lüders' lines in tension-torsion experiments on poly(vinyl chloride). *J. Polymer Sci.: Part A-2* **8,** 893–901.

Ben-Aoun, Z. and Pan, J. (1995). Influences of non-singular stresses on plane-stress near-tip fields for pressure-sensitive materials and applications to transformation toughened ceramics. *Int. J. Fract.* (submitted for publication).

Boyce, M. C., Parks, D. M. and Argon, A. S. (1988). Large inelastic deformation of glassy polymers. Part I: rate dependent constitutive model. *Mech. Mater.* **7,** 15–33.

Bowden, P. B. (1973). The yield behavior of glassy polymers. In *The Physics of Glassy Polymers* (Edited by R. N. Haward), pp. 279–339. John Wiley & Sons, New York.

Bowden, P. B. and Jukes, J. A. (1972). The plastic flow of isotropic polymers. *J. Mater. Sci.* **7,** 52–63.

Breuer, H., Haaf, F. and Stabenow, J. (1977). Stress-whitening and yielding mechanism of rubber-modified PVC. *J. Macromol. Sci.-Phys.* **B14,** 387–417.

Chen, I.-W. (1991). Model of transformation toughening in brittle materials. *J. Am. Ceram. Soc.* **74,** 2564–2572.

Chu, C.-C. and Needleman, A. (1980). Void nucleation effects in biaxially stretched sheets. *J. Eng. Mater. Tech.* **102,** 249–256.

Cox, T. B. and Low, J. R., Jr. (1974). An investigation of the plastic fracture of AISI 4340 and 18 Nickel-200 grade maraging steels. *Metall. Trans.* **5,** 1457–1470.

Dong, P. and Pan, J. (1991). Elastic–plastic analysis of cracks in pressure-sensitive materials. *Int. J. Solids Struct.* **28,** 1113–1127.

Drucker, D. C. and Prager, W. (1952). Soil mechanics and plastic analysis or limit design. *Quart. Appl. Math.* **10,** 157–165.

G'Sell, C. and Jonas, J. J. (1979). Determination of the plastic behaviour of solid polymers at constant true strain rate. *J. Mater. Sci.* **14,** 583–591.

Gurland, J. (1972). Observations on the fracture of cementite particles in a spheroidized 1.05% C steel deformed at room temperature. *Acta Metall.* **20,** 735–741.

Gurson, A. L. (1975). Plastic flow and fracture behavior of ductile materials incorporating void nucleation, growth and interaction. Ph.D. Thesis, Brown University.

Gurson, A. L. (1977). Continuum theory of ductile rupture by void growth : Part I—Yield criteria and flow rules for porous ductile media. *J. Eng. Mater. Tech.* **99,** 2–15.
Haghi, M. and Anand, L. (1992). A constitutive model for isotropic, porous, elastic–viscoplastic metal. *Mech. Mater.* **13,** 37–53.
Haward, R. N. (1973). The post-yield behavior of amorphous plastics. In *The Physics of Glassy Polymers* (Edited by R. N. Haward), pp. 340–393. John Wiley & Sons, New York.
Haward, R. N. (1993). Strain hardening of thermoplastics. *Macromolecules* **26,** 5860–5869.
Hibbitt, H. D., Karlsson, B. I. and Sorensen, E. P. (1992). ABAQUS User Manual, Version 4–9.
Hill, R. (1950). *The Mathematical Theory of Plasticity*. Oxford University Press.
Hill, R. (1962). Acceleration waves in solids. *J. Mech. Phys. Solids* **10,** 1–16.
Hom, C. L. and McMeeking, R. M. (1989). Void growth in elastic–plastic materials. *J. Appl. Mech.* **56,** 309–317.
Huang, Y. and Kinloch, A. J. (1992). Modelling of the toughening mechanisms in rubber-modified epoxy polymers. Part I : finite element analysis studies. *J. Mater. Sci.* **27,** 2753–2762.
Hutchinson, J. W. and Neale, K. W. (1983). Neck propagation. *J. Mech. Phys. Solids* **31,** 405–426.
Jeong, H.-Y. (1992). A macroscopic constitutive law for porous solids with pressure-sensitive matrices and its implications for plastic flow localization and crack-tip behavior. Ph.D. Thesis, The University of Michigan, Ann Arbor, Michigan.
Jeong, H.-Y. and Pan, J. (1992). The effects of rate sensitivity and plastic potential surface curvature on plastic flow localization in porous solids. *Int. J. Fract.* **56,** 317–332.
Jeong, H.-Y., Li, X.-W., Yee, A. F. and Pan, J. (1994). Slip lines in front of a round notch tip for pressure-sensitive materials. *Mech. Mater.* **19,** 29–38.
Kim, M. and Pan, J. (1994). Effects of non-singular stresses on crack-tip fields for pressure-sensitive materials. Part I : plane strain case. *Int. J. Fract.* **68,** 1–34.
Kinloch, A. J. and Young, R. J. (1983). *Fracture Behaviour of Polymers*. Elsevier Applied Science.
Kinloch, A. J., Finch, C. A. and Hashemi, S. (1987). Effects of segmental molecular mass between crosslinks of the matrix phase on the toughness of rubber-modified epoxies. *Polym. Comm.* **28,** 322–326.
Lazzeri, A. and Bucknall, C. B. (1993). Dilatational bands in rubber toughened polymers. *J. Mater. Sci.* **28,** 6799–6808.
Pan, J., Saje, M. and Needleman, A. (1983). Localization of deformation in rate sensitive porous plastic solids. *Int. J. Fract.* **21,** 261–278.
Parker, D. S., Sue, H.-J., Huang, J. and Yee, A. F. (1990). Toughening mechanisms in core-shell rubber modified polycarbonate. *Polymer* **31,** 2267–2277.
Pearson, R. A. and Yee, A. F. (1991). Influence of particle size and particle size distribution on toughening mechanisms in rubber-modified epoxies. *J. Mater. Sci.* **26,** 3828–3844.
Peirce, D., Shih, C. F. and Needleman, A. (1984). A tangent modulus method for rate dependent solids. *Computers & Structures* **18,** 875–887.
Rabinowtz, S., Ward, I. M. and Perry, J. S. C. (1970). The effect of hydrostatic pressure on the shear yield behavior of polymers. *J. Mater. Sci.* **5,** 29–39.
Ramsteiner, F. and Heckmann, W. (1985). Mode of deformation in rubber-modified polyamide. *Polym. Comm.* **26,** 199–200.
Reyes-Morel, P. E. and Chen, I.-W. (1988). Transformation plasticity of CeO_2-stabilized tetragonal zirconia polycrystals. I. Stress assistance and autocatalysis. *J. Am. Ceram. Soc.* **71,** 343–353.
Rice, J. R. (1976). The localization of plastic deformation. In *Proc. 14th Int. Cong. on Theoretical and Applied Mechanics* (Edited by W. T. Koiter), pp. 207–220. North-Holland, Delft.
Rudnicki, J. W. and Rice, J. R. (1975). Conditions for the localization of deformation in pressure-sensitive dilatant materials. *J. Mech. Phys. Solids* **23,** 371–394.
Sauer, J. A., Pae, K. D. and Bhateja, S. K. (1973). Influence of pressure on yield and fracture in polymers. *J. Macromol. Sci.-Phys.* **B8,** 631–654.
Saje, M., Pan, J. and Needleman, A. (1982). Void nucleation effects on shear localization in porous plastic solids. *Int. J. Fract.* **19,** 163–182.
Spitzig, W. A., Sober, R. J. and Richmond, O. (1975). Pressure dependence of yielding and associated volume expansion in tempered martensite. *Acta Metall.* **23,** 885–893.
Spitzig, W. A., Sober, R. J. and Richmond, O. (1976). The effect of hydrostatic pressure on the deformation behavior of maraging and HY-80 steels and its implications for plasticity theory. *Metall. Trans.* **7A,** 1703–1710.
Spitzig, W. A. and Richmond, O. (1979). Effect of hydrostatic pressure on the deformation behavior of polyethylene and polycarbonate in tension and compression. *Polym. Eng. Sci.* **19,** 1129–1139.
Sternstein, S. S. and Ongchin, L. (1969). Yield criteria for plastic deformation of glassy high polymers in general stress fields. *Am. Chem. Soc. Polym. Preprint* **10,** 1117–1124.
Sue, H.-J. (1992). Craze-like damage in a core-shell rubber-modified epoxy system. *J. Mater. Sci.* **27,** 3098–3107.
Tandon, G. P. and Weng, G. J. (1988). A theory of particle-reinforced plasticity. *J. Appl. Mech.* **55,** 126–135.
Timoshenko, S. P. and Goodier, J. N. (1951). *Theory of Elasticity*. McGraw-Hill, New York.
Tvergaard, V. (1981). Influence of voids on shear band instabilities under plane strain conditions. *Int. J. Fract.* **17,** 389–407.
Tvergaard, V. (1982). On localization in ductile materials containing spherical voids. *Int. J. Fract.* **18,** 237–252.
Van Stone, R. H., Merchant, R. H. and Low, J. R., Jr. (1974). Investigation of the plastic fracture of high-strength aluminum alloys. *ASTM STP* **556,** 93–124.
Yamamoto, H. (1978). Conditions for shear localization in the ductile fracture of void-containing materials. *Int. J. Fract.* **11,** 347–365.
Yee, A. F. and Pearson, R. A. (1986). Toughening mechanisms in elastomer-modified epoxies, Part 1. Mechanical studies. *J. Mater. Sci.* **21,** 2462–2474.
Yu, C.-S. and Shetty, D. (1989). Transformation zone shape, size, and crack-growth-resistance [R-curve] behavior of ceria–partially-stabilized zirconia polycrystals. *J. Am. Ceram. Soc.* **72,** 921–928.

APPENDIX 1. HYDROSTATIC YIELD STRESS FOR A SPHERICAL THICK-WALLED SHELL

Consider the spherical thick-walled shell shown in Fig. 1(a), where r represents the radial distance from the center, a represents the inner radius and b represents the outer radius of the shell. Suppose that the matrix of the shell is elastic–perfectly plastic and obeys Coulomb's yield criterion. Suppose also that the shell is subject to a radial traction Σ_m at $r = b$. The linear elastic solutions of the radial stress σ_{rr} and the hoop stress $\sigma_{\theta\theta}$ for the shell are (Timoshenko and Goodier, 1951)

$$\sigma_{rr} = \frac{\Sigma_m b^3 (r^3 - a^3)}{r^3 (b^3 - a^3)}, \tag{A1}$$

$$\sigma_{\theta\theta} = \frac{\Sigma_m b^3 (2r^3 + a^3)}{2r^3 (b^3 - a^3)}. \tag{A2}$$

Under spherically symmetric conditions, Coulomb's yield criterion can be written as

$$\sigma_{\theta\theta} - \sigma_{rr} + \mu' \frac{2\sigma_{\theta\theta} + \sigma_{rr}}{3} = \sigma_0. \tag{A3}$$

Substituting the elastic solutions of the radial stress and hoop stress in eqns (A1) and (A2) into the left side of eqn (A3), we have

$$\sigma_{\theta\theta} - \sigma_{rr} + \mu' \frac{2\sigma_{\theta\theta} + \sigma_{rr}}{3} = \frac{\Sigma_m b^3}{2(b^3 - a^3)} \left(\frac{3a^3}{r^3} + \mu' \right). \tag{A4}$$

The value of eqn (A4) increases as r decreases. This indicates that plastic deformation should start at the inner surface of the shell. The plastic zone spreads toward the outer surface with the increase of the radial traction Σ_m. Here we denote the radial stress at $r = c$ ($a \leqslant c \leqslant b$) as Σ_c when the plastic zone spreads to this radial distance $r = c$. Then the radial stress and hoop stress in the elastic region ($c \leqslant r \leqslant b$) are given as (Timoshenko and Goodier, 1951)

$$\sigma_{rr} = \frac{\Sigma_m b^3 (r^3 - c^3)}{r^3 (b^3 - c^3)} + \frac{\Sigma_c c^3 (b^3 - r^3)}{r^3 (b^3 - c^3)} \quad \text{for} \quad c \leqslant r \leqslant b, \tag{A5}$$

$$\sigma_{\theta\theta} = \frac{\Sigma_m b^3 (2r^3 + c^3)}{2r^3 (b^3 - c^3)} - \frac{\Sigma_c c^3 (2r^3 + b^3)}{2r^3 (b^3 - c^3)} \quad \text{for} \quad c \leqslant r \leqslant b. \tag{A6}$$

For the plastic region ($a \leqslant r \leqslant c$), the boundary conditions are

$$\sigma_{rr} = 0 \quad \text{at} \quad r = a, \tag{A7}$$

$$\sigma_{rr} = \Sigma_c \quad \text{at} \quad r = c. \tag{A8}$$

The equilibrium equation in the r direction gives

$$\frac{\partial \sigma_{rr}}{\partial r} = \frac{2(\sigma_{\theta\theta} - \sigma_{rr})}{r}. \tag{A9}$$

From eqns (A3), (A7)–(A9), we can obtain the radial and hoop stresses in the plastic region in terms of Σ_c as

$$\sigma_{rr} = \Sigma_c \frac{1 - (a/r)^{6\mu'/(3+2\mu')}}{1 - (a/c)^{6\mu'/(3+2\mu')}} \quad \text{for} \quad a \leqslant r \leqslant c, \tag{A10}$$

$$\sigma_{\theta\theta} = \Sigma_c \frac{3 - \mu'}{3 + 2\mu'} \frac{1 - (a/r)^{6\mu'/(3+2\mu')}}{1 - (a/c)^{6\mu'/(3+2\mu')}} + \frac{3\sigma_0}{3 + 2\mu'} \quad \text{for} \quad a \leqslant r \leqslant c, \tag{A11}$$

where Σ_c is

$$\Sigma_c = \frac{\sigma_0}{\mu'}[1-(a/c)^{6\mu'/(3+2\mu')}]. \tag{A12}$$

Once the plastic zone reaches the outer surface of the shell, the shell becomes fully yielded. Replacing c by b and Σ_c by $(\Sigma_m)_y$ in eqn (A12), we obtain the hydrostatic yield stress $(\Sigma_m)_y$ at the fully-yielded state as

$$(\Sigma_m)_y = \frac{\sigma_0}{\mu'}(1-f^{2\mu/(3+2\mu')}), \tag{A13}$$

where f $(=(a/b)^3)$ denotes the void volume fraction of the spherical shell. Equation (A13) also represents a hydrostatic yield stress for a spherical thick-walled shell of which the matrix is rigid–perfectly plastic. The solution given here is the generalization of the solution for the von Mises yield criterion in Hill (1950).

APPENDIX 2. PLASTIC POTENTIAL AND PLASTIC WORK EQUIVALENCE

For a pressure-sensitive matrix, Coulomb's yield function can be written as

$$\phi_c = \tau_e + \mu\sigma_m = \tau_o, \tag{A14}$$

where ϕ_c represents the yield surface in the stress space, τ_e represents the effective shear stress, μ represents the pressure sensitivity factor, σ_m represents the mean stress, and τ_o represents the generalized shear flow stress. With the assumption of normality, the plastic part of the rate of deformation tensor of the matrix, $\mathbf{d}^p$, is in the direction of the outward normal to the yield surface and can be written as

$$d^p_{ij} = \dot{\lambda}\frac{\partial\phi_c}{\partial\sigma^{ij}} \quad \text{or} \quad \mathbf{d}^p = \dot{\lambda}\left(\frac{\boldsymbol{\sigma}'}{2\tau_e}+\frac{\mu}{3}\mathbf{I}\right), \tag{A15}$$

where d^p_{ij} are the covariant components of $\mathbf{d}^p$, $\dot{\lambda}$ is a proportionality factor, σ^{ij} are the contravariant components of the Cauchy stress tensor $\boldsymbol{\sigma}$, and $\boldsymbol{\sigma}'$ is the deviatoric Cauchy stress tensor. It is easy to show that

$$\dot{\lambda} = \dot{\gamma}^p_e, \tag{A16}$$

where $\dot{\gamma}^p_e$ is the effective shear plastic strain rate of the matrix. The plastic dilatancy factor β is defined as the ratio of the volume increase rate $\mathrm{tr}(\mathbf{d}^p)$ to the effective shear plastic strain rate $\dot{\gamma}^p_e$:

$$\mathrm{tr}(\mathbf{d}^p) = \beta\dot{\gamma}^p_e. \tag{A17}$$

With the assumption of normality, we can show $\beta = \mu$ from eqns (A15)–(A17).

From eqns (A14) and (A17), a plastic potential function ϕ_p with a plastic dilatancy factor β can be defined as

$$\phi_p = \tau_e + \beta\sigma_m = \tau_p, \tag{A18}$$

where τ_p can be regarded as a fictitious generalized shear flow stress. In this case, the plastic part of the rate of deformation tensor, $\mathbf{d}^p$, becomes

$$\mathbf{d}^p = \dot{\gamma}^p_e\left(\frac{\boldsymbol{\sigma}'}{2\tau_e}+\frac{\beta}{3}\mathbf{I}\right). \tag{A19}$$

Moreover, the equivalence of plastic work rate for the matrix can be written as

$$\begin{aligned}\boldsymbol{\sigma}:\mathbf{d}^p &= (\tau_e+\beta\sigma_m)\dot{\gamma}^p_e \\ &= \tau_p\dot{\gamma}^p_e.\end{aligned} \tag{A20}$$

In the work of Gurson (1975, 1977), the macroscopic plastic work rate is assumed to be the plastic work rate of the matrix in an average sense for a porous material. This assumption in conjunction with eqn (A20) gives

$$\boldsymbol{\Sigma}:\mathbf{D}^p = (1-f)\tau_p\dot{\gamma}^p_e. \tag{A21}$$

We define $\sigma_p = \sqrt{3}\tau_p$, where σ_p can be regarded as a fictitious generalized tensile flow stress. Then we can rewrite eqn (A21) as

$$\boldsymbol{\Sigma} : \mathbf{D}^p = (1-f)\sigma_p \dot{\varepsilon}_e^p, \tag{A22}$$

where $\dot{\varepsilon}_e^p (= \dot{\gamma}_e^p/\sqrt{3})$ is the effective tensile plastic strain rate of the matrix.